Adaptive Neural Controller for Maximum Power Point Tracking Of Ten Parameter Fuel Cell Model

Naggar H. SAAD[1] **Ahmed A. El-SATTAR**[2]
[1]EPM Department, Faculty of Engineering, Ain Shams University, Cairo, Egypt.Email: naggar2hassan@yahoo.com)
[2]EPM Department, Faculty of Engineering, Ain Shams University, Cairo, Egypt. Email : aasattar2@yahoo.com)

Abd el-aziz M. MANSOUR[3]
[3]Department of Electrical Engineering, Police Academy, Cairo, Egypt. Email: zizo_mansour3000@yahoo.com)

Abstract*: Nonlinear characteristic and internal behavior of the Proton Exchange Membrane (PEM) Fuel Cells under different load conditions is of paramount importance. This paper presents an adaptive neural controller based on a back-propagation algorithm for maximum power control of PEM fuel cell system. The system consists of a buck-boost converter connected to the fuel cell. The adaptive neural controller receives the error and change of error signals as inputs during load changes and generates the DC-DC converter duty cycle. By using the inference, the duty ratio of the buck-boost converter is controlled so that the fuel cell can provide the maximum power. The ANN controller monitors also the temperature, the pressure and the cell voltage. In this paper the dynamic model for proton exchange membrane fuel cells using ten parameter model is used. The model has been implemented in MATLAB/SIMULINK. Both the double-layer charging effect and the thermodynamic characteristic inside the fuel cell are included in the model.*

Keywords**:** *Proton Exchange Membrane; Ten Parameter Model; Adaptive Neural Network Controller; Maximum Power Tracking.*

1. INTRODUCTION

Proton Exchange Membrane fuel cells show great promise for use as distributed generation sources. Compared with other DG technologies, such as wind and photovoltaic generation, PEM fuel cells have the advantage that they can be placed at any site in a distribution system, without geographic limitations, to achieve the best performance. Electric vehicles are another major application of PEM fuel cells. The increased desire for vehicles with less emission has made PEM fuel cells attractive for vehicular applications since they emit essentially no pollutants and have high-power density and quick start.

PEM fuel cells are good energy sources to provide reliable power at steady state. So the PEM fuel cells can decrease the demand of electric energy by using operating point which provides maximum power all the time. Since the current-voltage characteristic of the fuel cell is nonlinear, then the tracking control of the maximum power is a complicated problem. In order to overcome this problem, many tracking control strategies have been proposed such as in Perturbation [1]: An observe method is used to obtain maximum power for fuel cell in fuel cell/battery hybrid power system. In [2] a Maximum Efficiency Point Tracking (MEPT) algorithm based on the perturbation and observation method is proposed for finding the optimal air supply rate to maximize the net-power generation of FC system. An adaptive fuzzy logic controller for maximum power control of grid-connected solid oxide fuel cell system is presented in [3]. In this paper an adaptive neural controller based on a back-propagation algorithm is used to extract maximum power point from PEM fuel cell stack under partial load insertion and rejection test. Dynamic analysis of PEM fuel cell including thermodynamics of the cell and double layer charging effect by using ten parameter model is presented in simulation by "Matlab/Simulink". Partial load insertion and rejection test is presented to simulate the behavior of the PEM fuel cell under different loading conditions.

This paper is organized as following: The basic operation of the PEM fuel cell and the dynamic model to execute design and analysis of adaptive neural controller are derived in Section 2. The adaptive neural network controller is used to achieve maximum power which is described in Section 3. Simulation results from the PEM fuel cell system is presented in Section 4. Finally, the conclusion is stated in section 5.

2. Fuel Cell Basic Operation

A PEM fuel cell converts the chemical energy of fuel hydrogen (H_2) and oxidizer oxygen (O_2) in to electrical energy. The typical PEM fuel cell stack is illustrated in Fig. 1. On the side of the cell in Fig. 1(b), referred as anode, the fuel is supplied under certain pressure. The fuel for this model is a pure gas H_2. The fuel spreads through electrodes until reaches the catalytic layer of the anode where it reacts to form protons and electrons as described by equation 1.The protons are transferred through the electrolyte (solid membrane) to the catalytic layer of the cathode.

$$H_{2(g)} \rightarrow 2H^+ + 2e^- \quad (1)$$

On the other side of the cell, the oxidizer flows in the channels of the plate and it spreads through the electrode until it reaches the catalytic layer of the cathode. The oxygen is consumed with the protons and electrons and the product, liquid water, is produced with residual heat in the surface of the catalytic particles. The electrochemical reaction that happens in the cathode is:

$$2H^+ + \frac{1}{2}O_2 + 2e^- \rightarrow H_2O + heat \quad (2)$$

Then the full chemical fuel cell reaction is:

$$H_2 + \frac{1}{2}O_2 \rightarrow H_2O + heat + electrical\ energy \quad (3)$$

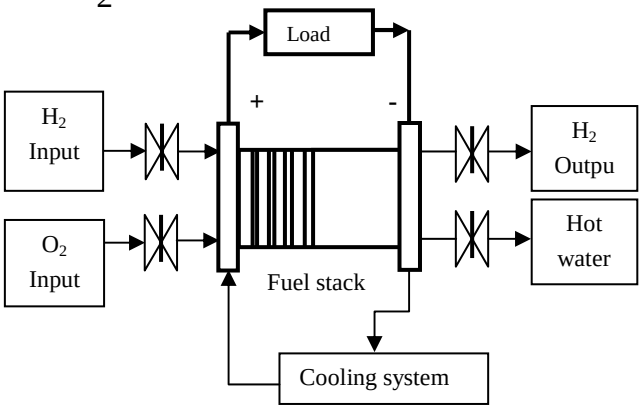

(a) Schematic diagram of fuel stack model

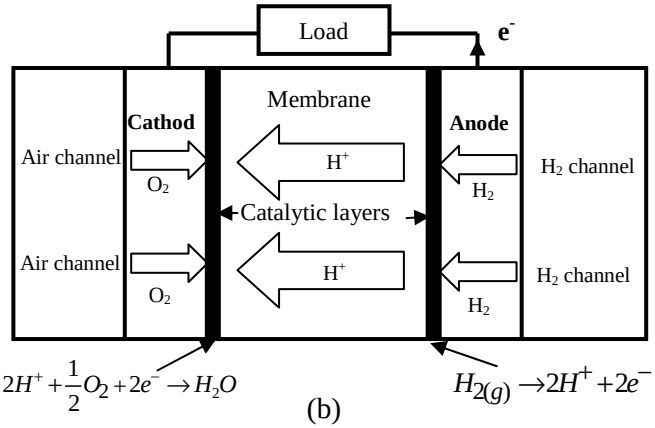

(b)

Fig. 1. (a) Schematic diagram of fuel stack model, (b) Fuel cell structure.

Ten Parameter Model

Ten parameter model is based on the following initial assumptions:

The chemical reactions in the polymeric membrane are instantaneous:

The voltage across the cell terminals is given by the following equation [4-8]:

$$v_{fc} = E_{Nernst} - v_{act} - v_{ohmic} - v_{conc} \quad (4)$$

In the equation (4), E_{Nernst} is the thermodynamic potential of the cell and it represents its reversible voltage, when losses are not considered in the process of electrical energy production without load. V_{act} is the activation voltage drop due to the activation of the anode and the cathode, V_{ohmic} is the ohmic voltage drop, a measure of the ohmic voltage associated with the conduction of the protons of solid electrolyte and internal electronic resistance and V_{conc} represents the voltage drop resulting of the concentration or transport of mass of oxygen and hydrogen. The Nernst voltage for given temperature T, oxygen pressure, P_{O2}, and hydrogen pressure, P_{H2}, is given by the following equation [7], [10]:

$$E_{Nernst} = 1.229 - 0.85\times10^{-3}(T - 298.15) + 4.3\times10^{-5}\times T\times\left[\ln(P_{H2}) + \frac{1}{2}\ln(P_{O2})\right] \quad (5)$$

The hydrogen and the oxygen partial pressures are calculated as in [7], [8].

The influence of fuel and oxidant delays on the fuel cell-output voltage during load transients can be written as [6]:

$$v_d = \lambda_e[i(t) - i(t) * \exp(-\frac{t}{\tau_e})] \quad (6)$$

Converting (6) to the Laplace domain, we obtain:

$$v_d(s) = \lambda_e I(s) \frac{\tau_e S}{\tau_e S + 1} \quad (7)$$

Where λ_e is constant factor, τ_e is the overall flow delay time and this voltage is considered to be subtracted from the right side of (5).

The activation voltage drop including anode and cathode can be calculated by [7], [10], and [11]:

$$v_{act} = -\left[\zeta_1 + \zeta_2 T + \zeta_3 T \ln(C_{O2}) + \zeta_4 T \ln(i_{fc})\right] \quad (8)$$

in which: i_{fc} is the stack current (A), T is the stack temperature (K), ζ_1, ζ_2, ζ_3 and ζ_4 are empirical coefficients given in table 1, A is the cell area (cm^2),C_{H2} is the hydrogen concentration in $mol.cm^{-3}$ and C_{O2} is the oxygen concentration on the cathode in $mol.cm^{-3}$ [4].

The ohmic voltage drop is given by:

$$v_{ohmic} = i_{fc}(R_m + R_c) \quad (9)$$

Where $R_m$is the equivalent resistance of the electron flow and R_c is the proton resistance considered as constant [1], [4]:

$$R_m = \frac{\rho_m L}{A} \quad (10)$$

In which L is the thickness of the membrane (cm), A is the membrane active area (cm^2) and ρ_m is the specific resistivity for the electrons flow (Ω.cm).

The concentration voltage drop can be calculated from the following equation:

$$v_{conc} = -m\exp(ni) \quad (11)$$

Where m and n are empirical coefficients [4], [11], i is the stack current density (A/cm^2).

Double-layer Charging Effect

In the PEM fuel cell, the two electrodes are separated by a solid membrane (Fig. 1(b)) which allows only the H^+ ions to pass, but blocks the electron flow. The electrons will flow from the anode through the external load and gather at the surface of the cathode, to which the protons of hydrogen will be attracted at the same time. Thus, two charged layers of opposite polarity are formed across the boundary between the porous cathode and the membrane. The layers, known as electrochemical double layer, can store electrical energy and behave like a super capacitor. The equivalent circuit of fuel cell considering this effect is given in Fig. 2. In this circuit, C is the equivalent capacitor due to the double-layer charging effect. Since the electrodes of a PEM fuel cell are porous; the capacitance C is very large and can be in the order of several Farads. R_{act} and R_{conc} are equivalent resistances of activation and concentration voltage drops.

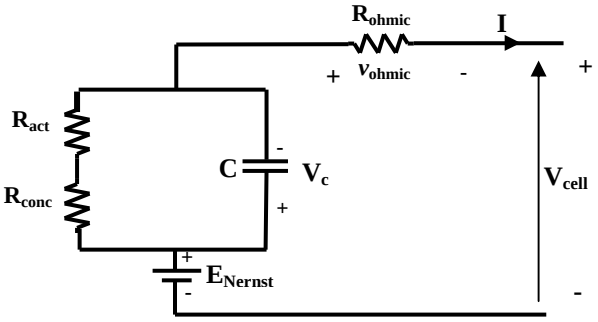

Fig. 2. Equivalent electrical circuit of the double-layer charging effect inside the PEM fuel cell.

The voltage across C is [9]:

$$V_c = (I - C\frac{dV_c}{dt})(R_{act} + R_{conc}) \quad (12)$$

The double-layer charging effect is integrated into the modeling, by using V_c instead of V_{act} and V_{conc} , to calculate V_{cell}.

The fuel-cell output voltage now turns out to be:

$$V_{cell} = E_{Nernst} - v_{ohmic} - V_c \quad (13)$$

And the stack fuel cell voltage can be calculated as:

$$V = N_{cell}\, V_{cell} \quad (14)$$

Where N_{cell} is the number of cells in the stack.

Thermodynamics of the fuel cell

During transitions, the temperature of the fuel cell will rise or drop according to the following equation [4], [6]:

$$C_t \frac{dT}{dt} = i(E_{Nernst} - V_{cell}) - H(T - T_f) \quad (15)$$

Where C_t is the thermal capacity of whole fuel cell volume, H is the thermal transmission coefficient for the whole fuel cell surface and T_f= 30+273.15° K.

The instantaneous electrical power supplied by the cell to the load can be determined by the equation [7]:

$$P_{FC} = V_{cell} \quad I \quad (16)$$

The FC efficiency can be calculated from the equation [7]:

$$\eta = \mu_f \frac{V_{cell}}{V_m} \quad (17)$$

Where μ_f is the fuel utilization coefficient, generally in the range of 95%.V_m is the maximum voltage that can be obtained using the Higher Heating Value (HHV) for the hydrogen enthalpy. The electrochemical potential (standard potential) corresponding to the HHV is 1.481 V per cell.

3. Adaptive Neural Network (ANN) Controller

Neural networks become indispensable tools in many areas of engineering and are continuing to receive much attention in Maximum Power Point Tracking (MPPT). An ANN controller, based on back-propagation algorithm, is used for maximum power point tracking. The input signals are the error (error between output voltage of the buck-boost converter and reference voltage) and the change of error, and the output signal is the duty cycle of the converter. The configuration of the proposed feed-forward neural network controller is shown in Fig. 3. The network consists of three layers: an input, a hidden, and an output layer. The numbers of nodes are two, four and one in the input, hidden and output layers respectively. The input signals are passed to the nodes in the hidden layer then to the output layer which provides the duty cycle of the buck-boost converter D. The sigmoid activation function is utilized in the hidden layer while the linear transfer function is utilized in the output layer. Learning process for ANNC is defined as change in connection weight values that result from capture of information. ANN learning is done using the backward propagation algorithm which cycles through two distinct passes, a forward pass followed by a backward pass through the layers of the network. Let us denote the weight of the connection from node i to node j by w_{ij} . The values of w_{ij} are initialized to small numbers in the range ±0.05. These weights are adjusted to new values in the backward pass. This phase begins with the computation of the error at each neuron in the output layer. The popular error function is the squared difference between the output of the node k o_k and the target value for that node y_k.

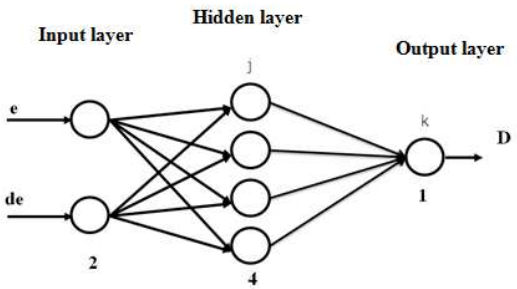

Fig. 3. Feed-forward neural network controller.

For each output layer node, the error term is computed as:

$$\delta_k = o_k(1-o_k)(y_k - o_k) \quad (18)$$

These errors are used to adjust the weights of the connections between the last-but-one layer of the network and the output layer. The new value of the weight w_{jk} of the connection from node j to node k is:

$$w_{jk}^{new}(n+1) = w_{jk}^{old}(n) + \Delta w_{jk}(n) \quad (19)$$

where, $\Delta w_{jk}(n)$ is the correction to the synaptic weight $w_{jk}^{old}(n)$ and is given as:

$$\Delta w_{jk}(n) = \eta_{jk}\, o_j(n)\, \delta_k(n) + \alpha\, \Delta w_{jk}(n-1) \quad (20)$$

Where η_{jk} is the learning rate, in the range of 0.1 to 0.9, α is the momentum constant and $\delta_k(n)$ is the local gradient.

4. Simulation Results

The fuel stack power system configuration is shown in Fig. 4. The system consists of fuel stack, DC-DC converter, load, and controller for MPPT (ANN controller). For validation of the model, the fuel stack model SR-12 modular PEM Generator was simulated. The parameters used for this simulation are presented in Table 1.

For the determination of the model characteristics, a load variation have been simulated in a given time range (namely 10000 seconds) leading the stack from a no load to a full load condition.

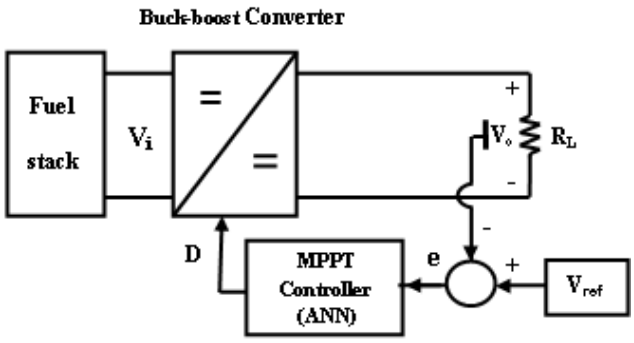

Fig. 4. Fuel stack power system configuration.

Fig. 5(a) shows the power – voltage-current curves of the stack with maximum power 1.07 KW versus current density Fig. 5(b) shows efficiency curve of the stack start from 79% at very low current density to 16% at high current density. .

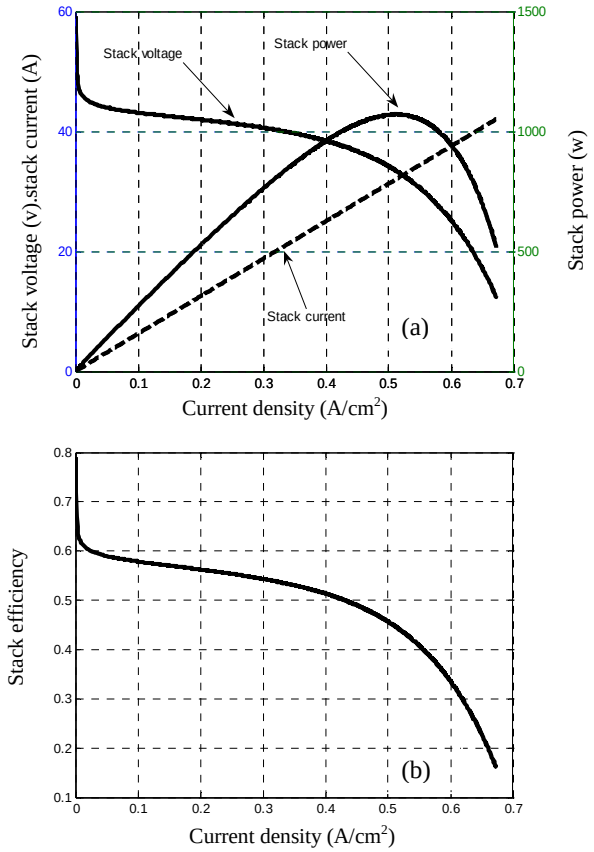

Fig. 5. Avista SR-12 PEM characteristics.

Maximum power tracking under partial load insertion and rejection test.

Fig. 6 depicts the load current for test of a partial load insertion followed by load rejection and shows the curve of the resulting voltage. Initially, the stack supplies 15 A to the load; after 5 seconds of simulation, the current is increased to 30 A, staying at this value until the simulation time reaches 10 seconds, the stack current is decreased to 15 A for another 5 seconds and increase again to 40 A in the same period. Finally, the load current is decreased again to 15 A until the end of the simulation (t = 25 seconds). It can be noticed that there is more response attenuation in the load insertion than in the load rejection, as expected. The values of the voltage are 38.58 V before the load increase, 34.52 V, and 31.55 V during the load pulses of 30A and 40A and, again, 38.58 V when the current is decreased. These values are obtained after having ceased the transient regime.

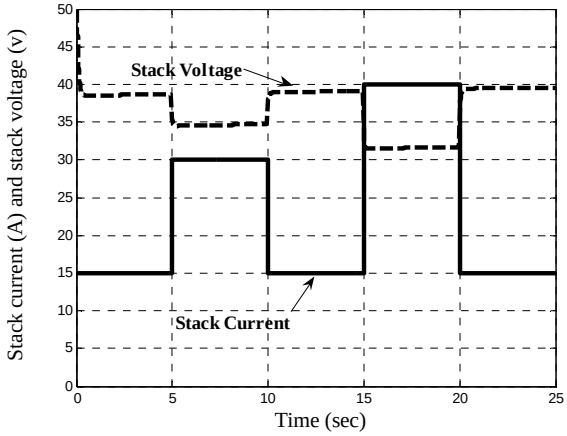

Fig. 6. Stack current and voltage for partial load insertion and rejection test.

Fig.7 presents the power response and the stack efficiency. A peak can be observed at the load insertion instant with a maximum value of 1362 W. When the load is decreased, the power presents a minimum value of 549W. The power steady state value is 579W for a current of 15A, 1038W for a current of 30A and 1262 W for a current 40A and the stack. The steady-state values for the efficiency are: 51.5% for a current of 15 A, 46 % for a current of 30 A and 42% for a current 40 A. It can be noticed that there is a significant reduction in the efficiency for variations of the demanded current, which should be taken into consideration when one evaluates a certain system.

Under partial load insertion we used an ANN controller to extract the maximum power from PEMFC stack as shown in Figs. 8 and 9. The output power of the stack by using ANNC under different load conditions is tracking the reference power as shown in Fig. 8. .

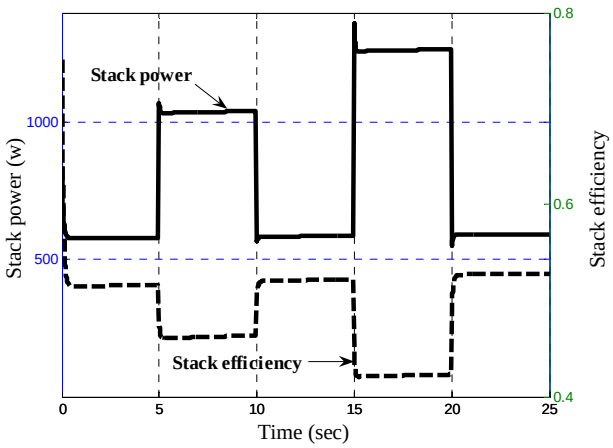

Fig.7. Stack power and efficiency for partial load.

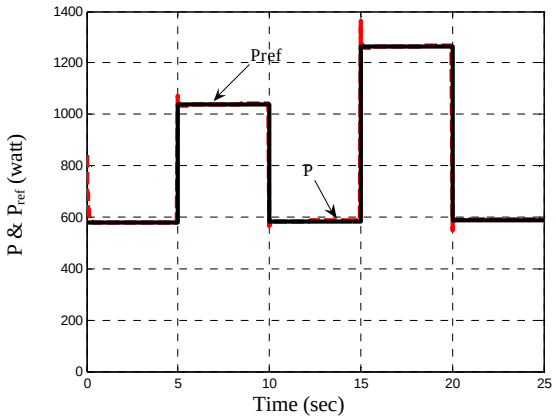

Fig. 8. Stack output and reference power for partial load using ANN controller.

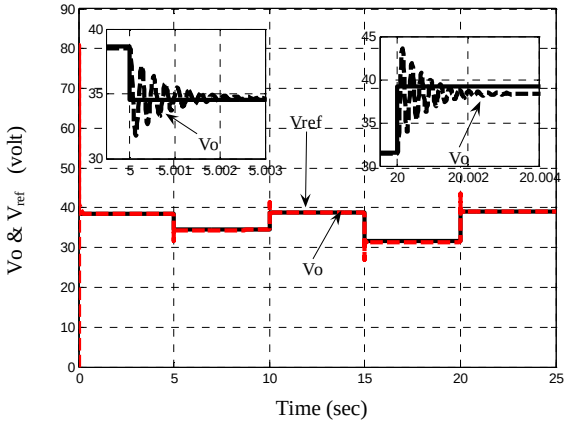

Fig. 9. Stack output and reference voltages.

The output voltage of the converter under different loading condition of the stack follows the reference voltage value corresponding to maximum power points of the stack as shown in Fig. 9.

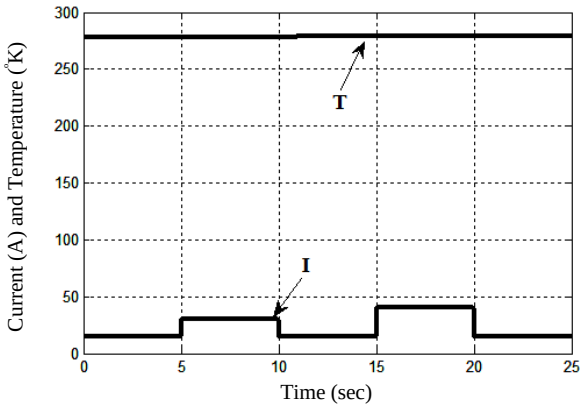

Fig. 10. Temperature of stack for partial load using ANN controller.

Fig. 10 monitors the temperature of fuel cell with ANN controller under different loading states. The controller keeps the temperature with range from 278°K to 279.2°K.

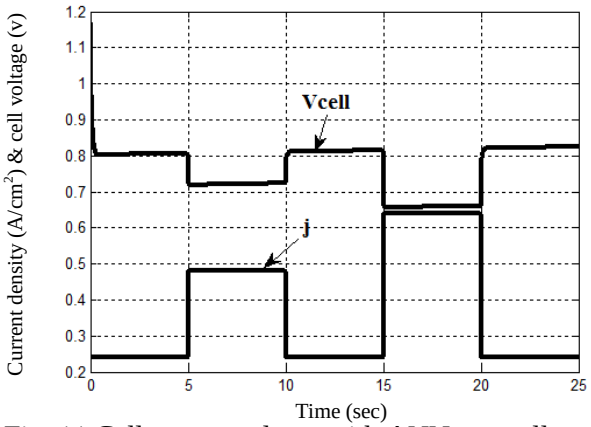

Fig. 11.Cell output voltage with ANN controller.

Fig.11 shows the change of voltage of cell with ANN controller under different loading conditions. The controller always keeps the cell voltage in range and tracking reference power and reference voltage.

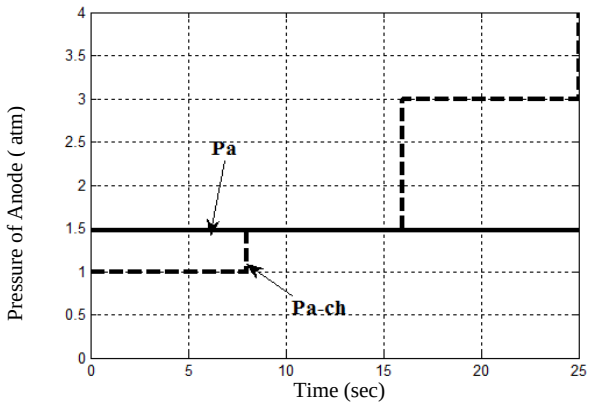

Fig. 12. Anode pressure for partial load with ANN.

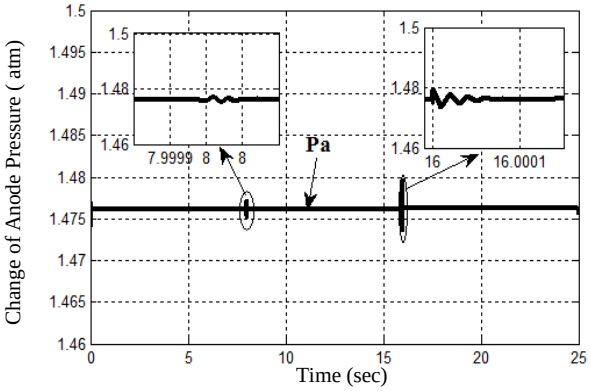

Fig. 13. Effect of load changing on anode pressure with ANN.

Figs. 12 and 13 depict the pressure of Anode with ANN controller under different loading and under change of inlet anode pressure from 1 to 3 atm in 25 sec. The controller is capable of keeping the pressure in permitted range within rated values.

5. **Conclusions**

This paper has presented maximum power tracking, of PEM fuel cell stack power system using adaptive feed-forward neural network controller based on back-propagation algorithm under partial load insertion and rejection test. The Ten parameter model is used for dynamic analysis of PEM fuel cell. As a matter of fact, the lower the parameter number is, the easier the simulations are, but at the same time, the gap respect to the real behavior of the real stack increases.

The partial and total load insertion and rejection tests demonstrated that the FC output voltage present a component which is directly related to the load current, known as the ohmic over-potential. This varies instantly with the variation of the current. There are still two other components which are the activation and the concentration over-potential, which are responsible for the attenuation of the voltage variation as a function of the current variation through the cell. Such dynamic voltage variation has significant reflexes on the supplied power. The simulated results show that the ANN controller is capable of tracking Maximum power point, temperature, pressure and voltage of the cell. The ANN controller gives a good performance for FC system with this type of converter under partial load conditions.

APPENDIX

Table (1) Parameters of the SR-12 Modular PEM Generator.

Param.	Value	Param	Value
T	323 k	n	48
A	62.5 cm^2	ζ_1	-0.948
L	25 μm	ζ_2	0.00286+0.0002 ln(*A*) +(4.3·10−5) ln(*CH*2)
P_{H2}	1.47628 atm	ζ_3	7.22e-5
P_{O2}	0.2095 atm	ζ_4	-1.0615e-4
R_C	0.0003 Ω	ψ	23
I_{max}	42 A	j_{max}	0.672 A/cm^2
C_t	22000	H	40
λ_e	0.0033	τ_e	80

REFERENCES

1. Dargahi M, Rouhi J, Rezanejad M and Shakeri M, "*Maximum Power Point Tracking for Fuel Cell in Fuel Cell/Battery Hybrid Power Systems*," European Journal of Scientific Research, 2009;Vol.25 No.4,p.538-548.
2. Nawapan Chanasut, Suttichai. P "*Maximum Power Control of Grid-Connected Solid Oxide Fuel Cell System Using Adaptive Fuzzy Logic Controller*," IEEE, 2008,p.1-6.
3. Jang Min-Ho, Lee Jae-Moon, Kim Jong-Hoon, Park Jong-Hu, and Cho Bo-Hyung "*Maximum Efficiency Point Tracking Algorithm Using Oxygen Access Ratio Control for Fuel Cell Systems*," Journal of Power Electronics, Vol. 11, No. 2, March 2011,p.194-201.
4. Bonanno D, Genduso F, Miceli R, member IEEE, Rando C "*Main Fuel Cells Mathematical Models: Comparison and Analysis in Terms of Free Parameters*," XIX International Conference on Electrical Machines Rome, ICEM 2010, p.1-6.
5. Xue D, Dong Z "*Optimal fuel cell system design considering functional performance and production costs*, "Journal of Power Sources ,1998, p.69-80.
6. Wang Caisheng, Nehrir M. Hashem, Shaw Steven R. , "*Dynamic Models and Model Validation for PEM Fuel Cells Using Electrical Circuits*," IEEE Transactions on energy Conversion, Vol. 20, NO. 2, June 2005, p.442-451.
7. Jeferson M. Correa, Felix A. Farret, Luciane N. Canah, "*An Analysis of the Dynamic Performance of Proton Exchange membrane Fuel Cells Using an electrochemical Model*" The 27th Annual Conference of the IEEE Industrial electronics Society, IEEE 2001;p.141-146.
8. Pathapati P.R., Xue X., Tang J., "*A new dynamic model for predicting transient phenomena in a PEM fuel cell system*," Renewable Energy, 2005;p.1-22.
9. José Javier San Martín, José Ignacio San Martín, Víctor Aperribay Iñigo Javier Oleagordia, Iñaki Martín, and José Mª Arrieta "*Technologies of PEM Fuel Cells and their application to LED semaphores and lighting systems*" international journal of computerVol.2,Issue.3,2008, p.248-258.
10. Springer T.E., Zawodzinski T.A., Gottesfeld S., "*Polymer electrolyte fuel cell model*," Journal of Electrochemicalsociety,1991;Vol. 138, NO. 8, 1991, p. 2334–2342.
11. Larminie J, Oxford, England. Dicks A, Brisbane, Australia "*Fuel Cell Systems Explained*" second edition, John Willey & Sons, chap. 3, January 2003.